Journal of Volcanology and Geothermal Research 304 (2015) 206–213

Contents lists available at ScienceDirect

Journal of Volcanology and Geothermal Research

journal homepage: www.elsevier.com/locate/jvolgeores

First determination of magma-derived gas emissions from Bromo volcano, eastern Java (Indonesia)

A. Aiuppa [a,b], P. Bani [c,d,*], Y. Moussallam [e], R. Di Napoli [a], P. Allard [f], H. Gunawan [c], M. Hendrasto [c], G. Tamburello [a]

[a] DiSTeM, Università di Palermo, Italy
[b] Istituto Nazionale di Geofisica e Vulcanologia, Palermo, Italy
[c] Center for Volcanology and Geological Hazard Mitigation, Jl. Diponegoro No 57, Bandung, Indonesia
[d] Laboratoire Magmas et Volcans, Univ. Blaise Pascale—CNRS—IRD, OPGC, 63000 Clermont-Ferrand, France
[e] Department of Earth Sciences, University of Cambridge, Downing Street, Cambridge CB2 3EQ, UK
[f] Institut de Physique du Globe de Paris, UMR7154 CNRS, 75005 Paris, France

ARTICLE INFO

Article history:
Received 12 April 2015
Accepted 2 September 2015
Available online 10 September 2015

Keywords:
Bromo volcano
Volcanic gases
SO_2 and CO_2 fluxes
Tengger Caldera
Eastern Java, Indonesia
Multi-GAS

ABSTRACT

The composition and fluxes of volcanic gases released by persistent open-vent degassing at Bromo Volcano, east Java (Indonesia), were characterised in September 2014 from both in-situ Multi-GAS analysis and remote spectroscopic (dual UV camera) measurements of volcanic plume emissions. Our results demonstrate that Bromo volcanic gas is water-rich (H_2O/SO_2 ratios of 56–160) and has CO_2/SO_2 (4.1 ± 0.7) and CO_2/S_{tot} (3.2 ± 0.7) ratios within the compositional range of other high-temperature magma-derived gases in Indonesia. H_2/H_2O and H_2S/SO_2 ratios constrain a magmatic gas source with minimal temperature of ~700 °C and oxygen fugacity of 10^{-17}–10^{-18} bars. UV camera sensing on September 20 and 21, 2014 indicates a steady daily mean SO_2 output of 166 ± 38 t d^{-1}, which is ten times higher than reported from few previous studies. Our results indicate that Bromo ranks amongst the strongest sources of quiescent volcanic SO_2 emission measured to date in Indonesia, being comparable to Merapi volcano in central Java. By combining our results for the gas composition with the SO_2 plume flux, we assess for the first time the fluxes of H_2O (4725 ± 2292 t d^{-1}), CO_2 (466 ± 83 t d^{-1}), H_2S (25 ± 12 t d^{-1}) and H_2 (1.1 ± 0.8) from Bromo. Our study thus contributes a new piece of information to the still limited data base for volcanic gas emissions in Indonesia, and confirms that much remain to be done to fully assess the contribution of this very active arc region to global volcanic gas fluxes.

1. Introduction

The Indonesian volcanic arc, extending from west Sumatra to Sulawesi in the northeast, hosts 140 identified active volcanoes (Global Volcanism Program, http://www.volcano.si.edu/), ~100 of which have erupted in the recent history (Simkin and Siebert, 1994). Indonesia is one of the most active volcanic regions on our planet, and paid a prominent tribute to the historical death toll from volcanism. Paradoxically, however, relatively little is known about the contribution of the Indonesian island arc to the global volcanic gas fluxes to the atmosphere (see Oppenheimer et al., 2014). In their reference compilation of volcanic SO_2 fluxes, Andres and Kasgnoc (1998) reported data for only 4 continuously degassing volcanoes in Indonesia (Merapi, Galunggung, Bromo and Slamet), whose single cumulative contribution (~0.1 Tg yr^{-1}) cannot account for the overall country's contribution to the global volcanic SO_2 budget (recently estimated as 10-18 Tg/yr by different authors; see Oppenheimer et al., 2014 for a review). Attempts to extrapolate from these few available data have led to estimates of a regional SO_2 flux that span more than one order of magnitude, from 0.12–0.18 Tg/yr (Hilton et al., 2002) to 3.5 Tg/yr (Nho et al., 1996). The latter figure also includes the contribution of eruptive degassing to the SO_2 budget. Syn-eruptive emissions in Indonesia were determined for only a few events, from either space-borne sensing or the petrologic method (see Pfeffer, 2007, for an updated list), but the total (passive + eruptive) SO_2 budget does not results better constrained (0.48–3.8 Tg/yr; Pfeffer, 2007) than that for only passive emissions. This paucity of information has persisted until today (see Shinohara, 2013), even though a recent work by Bani et al. (2013) provided the first SO_2 flux datum for Papandayan and further data for Bromo volcanoes in Java.

Our current knowledge for volcanic degassing in Indonesia is even more lacking for other major volcanic gas species such as H_2O and CO_2, whose emission rates were quantified at only one single volcano, Merapi in central Java (Allard et al., 1995, 2011; Toutain et al., 2009). Published volcanic gas analyses are available for only ~10 Indonesian volcanoes (compiled in Pfeffer, 2007), which makes quantifying regional gas flux inventories very problematic. For instance, Hilton et al. (2002) estimated an Indonesian CO_2 flux of ~0.36 Tg/yr that is poorly

* Corresponding author at: Laboratoire Magmas et Volcans, Univ. Blaise Pascale—CNRS—IRD, OPGC, 63000 Clermont-Ferrand, France.
E-mail address: philipson.bani@ird.fr (P. Bani).

http://dx.doi.org/10.1016/j.jvolgeores.2015.09.008
0377-0273/

constrained from very few data. In summary, given the intense volcanic activity in Indonesia and the important gas emissions sustained by other arc segments in the southwest Pacific, such as Papua New Guinea (McGonigle et al., 2004; McCormick et al., 2012) and Vanuatu (Bani et al., 2012), increasing the data base for volcanic gas compositions and fluxes in Indonesia is essential to refining current global volcanic gas inventories (Hilton et al., 2002; Burton et al., 2013; Shinohara, 2013).

Bromo volcano, a small pyroclastic cone inside the wide Tengger Caldera in eastern Java (Fig. 1), has been one of the most active volcanoes of Indonesia in historical time (GVP), displaying persistent plume emissions via open-vent degassing from its summit crater (Fig. 1c) and occasional eruptions (the last one in January-March 2011; GVP, 2012). This volcano has been studied on a few rare occasions from the ground for its SO_2 emission and considered to be a small emitter (Andres and Kasgnoc, 1998; Bani et al., 2013). However, satellite records in 2011–2013 have revealed that Bromo, in tandem with nearby Semeru volcano (Fig. 1d), ranks in the top-20 list of degassing volcanoes on Earth (Carn et al., 2014). Therefore, further ground-truth information is badly needed for better assessing its actual SO_2 flux contribution, but also the composition of its volcanic gases which have never been studied. This was the aim of our present work.

We here report on the results of a field survey performed in September 2014, during which the chemical composition of Bromo's volcanic gas plume was characterised using a Multi-component Gas Analyser System (Multi-GAS; Aiuppa et al., 2005; Shinohara, 2005). The volcanic SO_2 flux was also simultaneously determined using a dual-UV camera system (Tamburello et al., 2012). Combining the two data types allows us to provide the volatile emission budget for H_2O, CO_2, SO_2, H_2S and H_2 from Bromo volcano.

2. Bromo volcano

Bromo (Latitude 7.942°S; Longitude 112.95°E) is a small tuff cone located in the central part of the Tengger caldera, a large (16-km-wide) polygenetic depression topping the summit of the (820 kyr old) Tengger volcanic massif in east Java (van Gerven and Pichler, 1995) (Fig. 1a–b). Bromo is the only active centre of a cluster of post-caldera

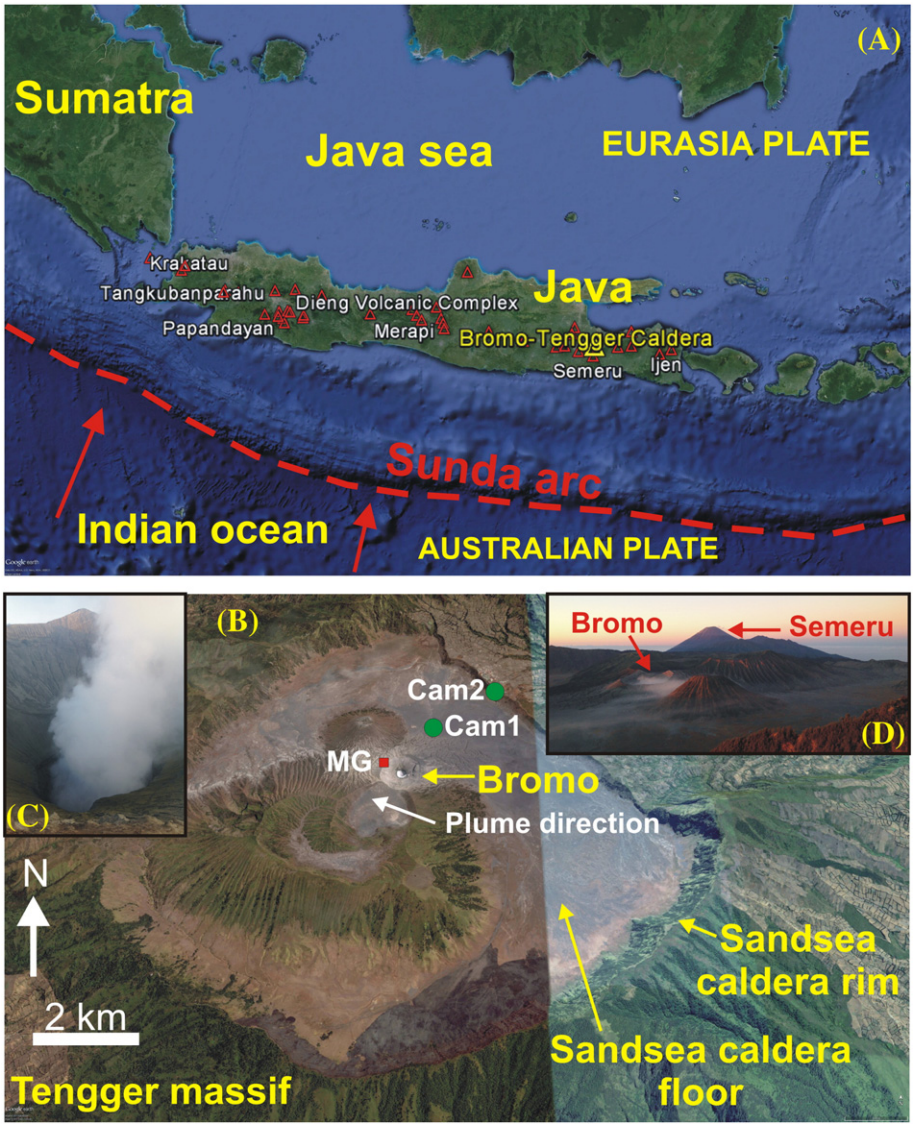

Fig. 1. (A) Map of Java island (source: Googleearthpro), showing the location of the most active Indonesian volcanoes (source: GVP) and of Bromo volcano on east Java. Volcanism in Java is related to subduction of the Australian Plate underneath the Eurasia Plate along the Sunda arc (the main direction of plate convergence is shown by red arrows); (B) Googleearthpro map of the Tengger caldera summit, showing the location of Bromo volcano. The red square (MG) indicates the position of the Multi-GAS, while the green circles stand for the positions of the UV camera on 20 September (Cam1) and 21 September (Cam2). Insets (C) and (D) are photos showing open-vent activity on Bromo's summit and a sunrise view of Bromo and Semeru volcanoes in the Tengger caldera, respectively.

cones constructed on the floor of the Sandsea caldera, the youngest (late Pleistocene to early Holocene) and smallest (9 × 10 km) collapse structure of the Tengger volcanic complex (Fig. 1b). van Gerven and Pichler (1995) distinguish five stages in the evolution of the Tengger system, and consider that intra-caldera (Bromo) activity started sometimes prior to ~1800 yrs B.P.. More than 60 explosive eruptions (mainly of VEI = 2) have occurred at Bromo over the past four centuries, most recently in 2000–2001, 2004, and 2010–2012 (GVP; CVGHM Reports). In spite of this recurrent activity, available information on Bromo in the international geological literature is relatively scarce. Mulyadi (1992) and van Gerven and Pichler (1995) discuss some aspects of the structural and geological evolution of the Tengger system. The petrology of erupted magmas (medium- to high-k andesites and basaltic andesites) is described in Whitford et al. (1979), van Gerven and Pichler (1995) and, marginally, in the study of Carn and Pyle (2001) on the nearby Lamongan Volcanic Field. Gottschämmer (1999) and Gottschämmer and Surono (2000) describe the location and spectral characteristics of the volcano seismicity (tremor, shock waves and LP events). Andres and Kasgnoc (1998) report a SO_2 flux of only of 14 t d^{-1} from Bromo, based on COSPEC measurements in 1995.

3. Material and methods

Our gas measurements on Bromo were carried out on 20–21 September, 2014. Intense, passive open-vent degassing was occurring at that time (Fig. 1c), in synchronism with a broad intensification of both volcanic activity and seismicity initiated in April–May 2014, which led local authorities to increase the Volcanic Alert Level to 2 (on a scale of 1–4; source: Pusat Vulkanologi dan Mitigasi Bencana Geologi, PVMBG).

A compact, portable version of the INGV-type Multi-GAS (same as in Aiuppa et al., 2012, 2013) was temporarily deployed during the two consecutive days on the rim of Bromo's summit crater (Fig. 1b) in order to measure at 0.5 Hz frequency the in-plume concentrations of volcanic gas species. The Multi-GAS was powered by a small (6 Ah) 12 V LiPo internal battery and mounted onboard the same sensor kit as in Aiuppa et al (2013). H_2O and CO_2 were detected by near dispersive infra-red spectroscopy (Licor LI-840A; 0–60,000 ppm range), and SO_2, H_2S and H_2 via specific electrochemical sensors (respectively, models 3ST/F, EZ3H, and EZT3HYT "Easy Cal"; all from City Technology a with calibration range of 0–200 ppm). All the signals were co-acquired and stored in a data-logger, then post-processed using the Ratiocalc software (https://sites.google.com/site/giancarlotamburello/volcanology/ratiocalc; Tamburello (2015)), as described in Aiuppa et al. (2014). Uncertainties in derived gas ratios (Table 1) are typically ≤10%, except for H_2O/SO_2 (≤30%).

High-rate (0.5 Hz) SO_2 flux time-series were also obtained in both days using the dual UV camera technique (Kantzas et al., 2010; Tamburello et al., 2012; see Burton et al., 2015 for a recent review of UV-camera applications in volcanology). The dual UV camera technique is a modified version of the original UV-camera method of (Mori and Burton, 2006), and uses two co-aligned cameras (in this specific case: two Apogee Instruments Alta U260 cameras, each fitted with a16 bit 512-512 pixel Kodak KAF-0261E thermo-electrically cooled CCD array detector). The advantage of using two simultaneously acquiring cameras, instead of only one camera with two switching filters (as in the original Mori and Burton, 2006 paper), is the higher time resolution, and the ability to more effectively manage errors arising from broad band absorption e.g., aerosols and ash (Kantzas et al., 2010; Kern et al., 2010, 2013). The same hardware as in Tamburello et al. (2012) was used here. A Pentax B2528-UV lens (f = 25 mm; field-of-view of 24°) was mounted to the fore of each camera. Filters (of 10 nm FWHM; Asahibunko Inc.) were placed over each of these lenses, being centred on 310 nm (affected by plume SO_2 absorption) and on 330 nm (falling outside the SO_2 absorption bands), respectively. Absorbance A, per each camera pixel and each couple of co-acquired images, was thus calculated as:

$$A = -\log_{10}[(IP_{310}/IB_{310})/(IP_{330}/IB_{330})] \quad (1)$$

where IP and IB are the dark image subtracted plume and background sky images, with the subscripted filters in place. Absorbance was converted into SO_2 column amount by a calibration procedure achieved using 4 SO_2 cells of known concentration (path amounts of 94, 189, 475, and 982 ppm m). Cells were sequentially placed in front of each camera when pointing to the background sky above the plume at the beginning of each measurement series. Having the sun behind cameras minimised the spectral intensity changes during measurements and calibrations. Data were post-processed using Vulcamera software (Tamburello et al., 2011) that also allows calculating the plume transport speeds using cross-correlation analysis (Tamburello et al., 2012, 2013). Given the short distance from the volcano target, the relatively well constrained plume transport speed (Table 2), and the plume typically appearing transparent and with no visible ash, all conditions at which UV-camera errors are minimised (Kern et al., 2010, 2013), we evaluate the uncertainty in the UV camera measurements at ≤25%. In such optical conditions, good correspondence between results of DOAS (differential optical absorption) scanning spectrometers and UV cameras has also been demonstrated (Kantzas et al., 2010).

4. Results

During most of our measuring period, the volcanic plume was seen to convectively rise from the bottom of Bromo crater (Fig. 1c), before being dispersed by gentle easterly winds (see below) towards the north-western outer rim where the Multi-GAS was deployed (Fig. 1b). The air-diluted volcanic plume was buoyant enough to float above the crater rim for a large part of time, but could be pumped into our Multi-GAS sensor during four successive time periods (referred to as A to D in Fig. 2 and Table 1). Distinct increases in the volcanic gas mixing ratios were accurately detected during these four intervals (Fig. 2). The peak in-plume mixing ratios resulted to be 460 ppmv (CO_2), 16 ppmv (SO_2), 6.7 ppmv (H_2S), 4.6 ppmv (H_2) and ~2000 ppmv (H_2O), the latter being corrected for an ambient air mean H_2O mixing ratio of 19,300 ppmv. Strong positive co-variations observed between SO_2 and the other detected volatiles (Fig. 2) confirm their common volcanic origin. From these correlations, the gas/SO_2 molar plume ratios for each recording interval were obtained by calculating the gradients of the

Table 1
Volatile ratios calculated for the 4 distinct intervals (A–D) in Fig. 2. The arithmetic mean and standard deviation (σ) of the 4 observations is also shown.

	A		B		C		D		Mean	
	20.9.14 morning		20.9.14 afternoon		21.9.14 morning		21.9.14 afternoon			
	Mean	σ	Mean	σ	Mean	σ	Mean	σ		σ
H_2O/SO_2	56 ± 16		66 ± 17		160 ± 55		123 ± 54		**101** ± 49	
CO_2/SO_2	3.4 ± 0.6		3.8 ± 1.5		5.1 ± 1.8		4.1 ± 1.9		**4.1** ± 0.7	
H_2S/SO_2	0.26 ± 0.10		0.44 ± 0.05		0.20 ± 0.07		0.15 ± 0.10		**0.26** ± 0.1	
H_2/SO_2	0.13 ± 0.05		0.15 ± 0.05		0.39 ± 0.22		0.19 ± 0.13		**0.22** ± 0.1	

Table 2
Volatile fluxes from Bromo volcano.

	20.9.14[a] morning	21.9.14[b] morning	Average[c] (20–21 Sept)
	Mean ± σ	Mean ± σ	Mean ± σ
Plume speed (m/s)[d]	8.0 ± 1.8	4.6 ± 1	
Fluxes (tons/day)[e]			
SO_2	168 ± 35	164 ± 70	**166** ± 37.5
H_2O	2628 ± 773	7383 ± 2540	**4725** ± 2292
CO_2	393 ± 69	574 ± 203	**466** ± 83
H_2S	25 ± 9	17 ± 6	**25** ± 12
H_2	0.7 ± 0.5	2 ± 1	**1.1** ± 0.8

[a] Fluxes calculated from gas composition measured in interval A (Table 1).
[b] Fluxes calculated from gas composition measured in interval C (Table 1).
[c] Fluxes calculated from the "mean" gas composition of (Table 1) and the mean SO_2 flux of 166 tons/day.
[d] Measured with UV cameras.
[e] Calculated by multiplying the SO_2 flux by MultiGAS-derived compositions.

best-fit regression lines (shown in Fig. 2 with the relative equations). The resulting ratios are listed in Table 1.

H_2O was a factor ~100 more abundant than SO_2 in Bromo plume on average (Fig. 2a). H_2O/SO_2 ratios fluctuated in the different recording intervals (range from 56 to 160; Fig. 2a and Table 1). This variability (about ±60% of the mean) is well above the typical associated measurement errors (±30%), and suggests a real temporal fluctuation of the gas source. Instead, the CO_2/SO_2 molar ratio showed a much greater temporal stability, ranging from 3.4 to 5.1 and with a mean of 4.1 ± 0.7 (Fig. 2b). While the concentrations of the minor gas components H_2S and H_2 exhibited significant temporal variability (Fig. 2c and d), the H_2S/SO_2 and H_2/SO_2 ratios have quite well defined average values of 0.26 ± 0.1 (range: 0.15–0.44) and 0.22 ± 0.1 (range: 0.13–0.4), respectively. We thus derive a mean H_2/H_2O ratio of ~0.002, comparable to the ratios observed at other open-vent degassing volcanoes such as Etna in Italy (Aiuppa et al., 2011) and Gorely in Kamchatka (Aiuppa et al., 2012) (Fig. 3).

The SO_2 flux was measured for ~2 consecutive hours on both September 20 and 21. For the two distinct days, the calculated plume transport speed (averaging at 8.0 ± 1.8 and 4.6 ± 1 m/s) and UV-camera positions are shown in Table 2 and Fig. 1b, respectively. In both measurement days, observations were limited to the early morning clear-sky conditions (8–10 and 9–11 am local time, respectively), when the plume typically appeared transparent. Later in the day, visibility was rapidly reduced by either meteorological clouds or by the plume becoming too condensed. An example of a clear-sky UV camera image of the SO_2-rich Bromo plume is illustrated in Fig. 4a. The pseudo-colour contours show that SO_2 column amounts up to ~600 ppm m were detected in the core of the plume at its exit from the crater rim. The SO_2 flux was calculated by integrating along a slant column amount profile, roughly perpendicular to the plume transport direction (e.g., cross section L–R in Fig. 4a), then by scaling to the plume transport speed. Processing sequences of images allowed us to derive time-series of SO_2 fluxes at 0.5 Hz, an example of which (for the September 20 dataset) is illustrated in Fig. 4b. The diagram demonstrates the oscillatory nature of volcanic degassing at Bromo, with 60–120 s long pulses of SO_2 emission that repeated at an average periodicity of a few minutes. This observation reminds analogue degassing features observed at both Etna and Stromboli open-vent basaltic volcanoes (Tamburello et al., 2013) and provides insight into the degassing mechanism at Bromo. The time-averaged SO_2 flux was very steady as 1.94 kg/s and 1.90 kg/s during the two days of our measurements, leading to a mean daily output of 166 ± 38 tons d^{-1} (Table 2).

5. Discussion

We provide here the first data set for the chemical composition of gas emissions supplied by open-vent magma degassing at Bromo

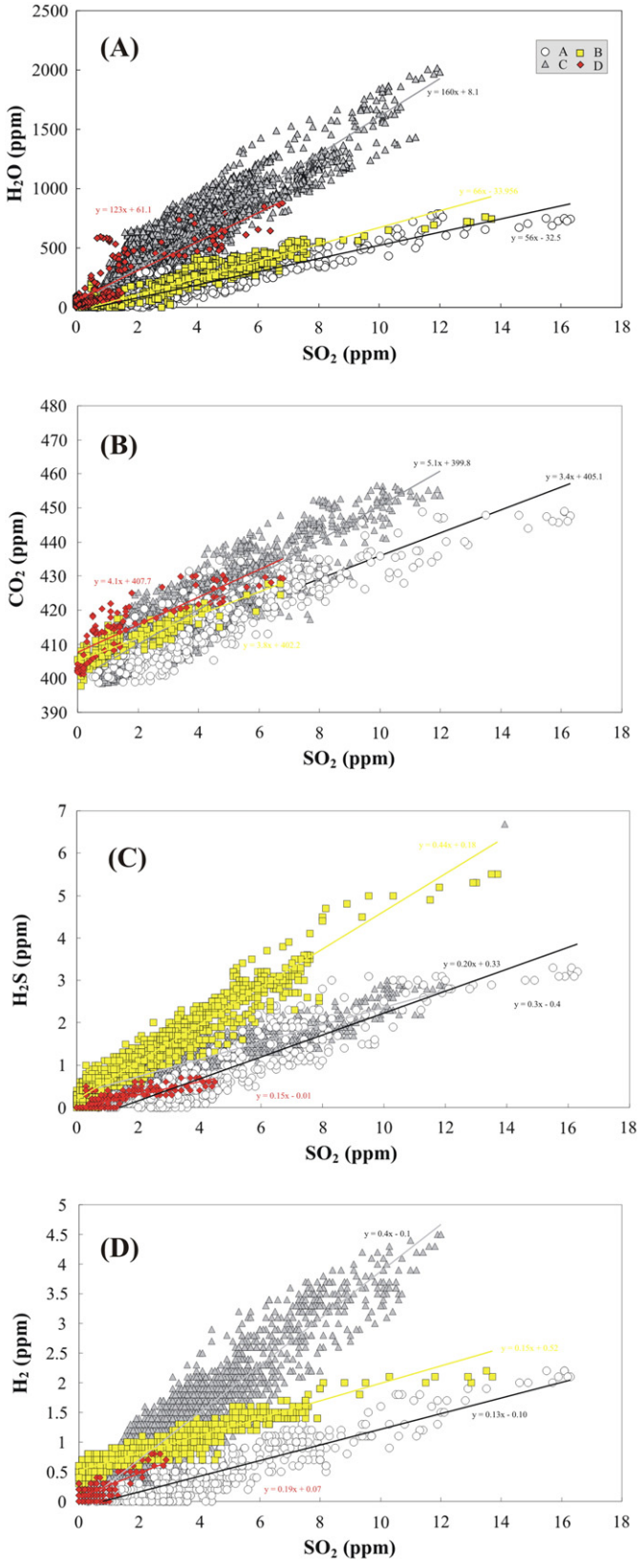

Fig. 2. Scatter plots of SO_2 vs (A) H_2O (B) CO_2 (C) H_2S and (D) H_2 mixing ratios in the Bromo plume. H_2O mixing ratios are after subtraction of a mean ambient air H_2O mixing ratio of 19,300 ppmv (measured by the Multi-GAS in the background site Cam1; see Fig. 1). Data acquired in the four distinct fumigation events A–D are distinguished by different symbols (see legend). The best-fit regression lines, and their respective equations, are separately shown (in each of the 4 plots) for periods A–D. The slopes of these regression lines are the averaged volatile/SO_2 ratios during each interval (reported in Table 1).

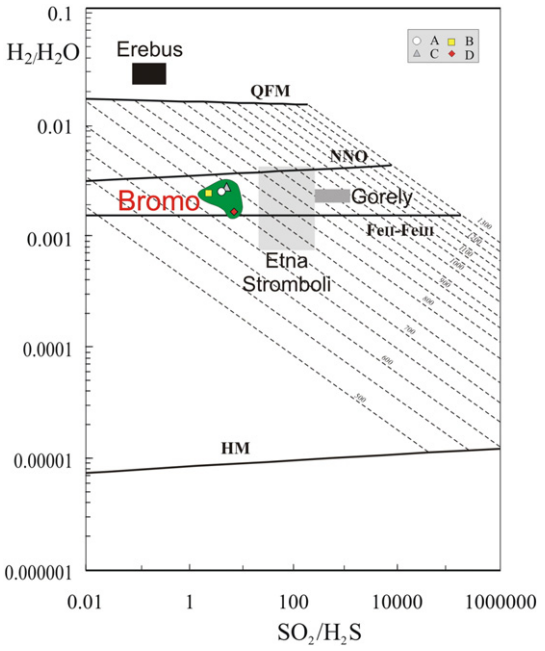

Fig. 3. Scatter plot of SO_2/H_2S vs H_2/H_2O ratios in the Bromo plume (calculated for the 4 fumigation intervals from data in Table 1). The compositional fields of other open-vent volcanoes are shown for comparison (data source: Etna-Stromboli, Aiuppa et al., 2011; Erebus, Moussallam et al., 2012; Gorely, Aiuppa et al., 2012). The solid lines are equilibrium SO_2/H_2S and H_2/H_2O ratios in magmatic gases, calculated at 0.1 MPa pressure and in a range of temperatures (isotherms are shown in the figure as dashed lines) and redox conditions. The model lines labelled QFM, NNO, HM and $Fe^{II}Fe^{III}$ stand for equilibrium compositions at the fO_2–temperature dependences fixed by the rock buffers Quartz–Fayalite–Magnetite, Nickel–Nickel oxide, hematite–magnetite, and Fe(II)–Fe(III) (see Aiuppa et al., 2011 for details on the calculations of the model lines). The SO_2/H_2S vs H_2/H_2O ratios in the Bromo plume are consistent with a quenched equilibrium gas composition at a temperature of ~700 °C and redox conditions intermediate between Fe_{II}–Fe_{III} (NNO) and Nickel–Nickel Oxide buffers.

volcano. This volcano, while site of visible, persistent degassing over the last decade, has received little attention until present.

Our Multi-GAS-sensed compositions demonstrate a H_2O-rich nature of Bromo volcanic gases. The mean H_2O/SO_2 ratio of 101 ± 49 (Table 1) falls within the upper domain for arc volcanic gases (Fischer, 2008; Shinohara, 2013). Considering that our results approximate for the bulk composition of Bromo volcanic gas (excepting halogen compounds), the gas ratios in Table 1 constrain the mol.% chemical composition of the gas. One obtains an H_2O molar proportion of 94.8%, which is still in the typical arc range (Fischer, 2008). However, the majority of open-vent, mafic arc volcanoes, similar in nature to Bromo, emit somewhat less hydrous gases, with H_2O/SO_2 ratio clustering at ~50 and H_2O at ~93 mol% (see the reviews of Shinohara, 2013; Aiuppa, 2015). We find that Bromo volcanic gas closely matches these values on September 20 (intervals A–B, H_2O/SO_2 ratios at ~56–66), but not on the following day when the H_2O/SO_2 ratio was about twice higher (123–160; Table 1). We cannot exclude, therefore, that about a half of H_2O measured on September 21 was not magmatic in origin, and derived from an external source such as re-evaporated meteoric water. The large meteoric precipitation events that occurred on the Tengger massif on the night between 20 and 21 September support this conclusion.

The mean CO_2/SO_2 ratio of 4.1 (Table 1) of Bromo volcanic gas, combined with a H_2S/SO_2 ratio of ~0.26, corresponds to a mean CO_2/S_t ratio of 3.2 (range 2.6–4.2; where $S_t = SO_2 + H_2S$). Comparing with available gas data for Indonesian volcanoes (Fig. 5), we find that our mean Bromo volcanic gas ratio of 3.2 is well below the CO_2/S_t ratios that characterise the majority of close-to-boiling hydrothermal gases in Indonesia (see Fig. 5). The prevailingly high CO_2/S_t signature of these latter manifestations reflects preferential sulphur scrubbing by gas–water–rock reactions at hydrothermal conditions (Symonds et al., 2001) (see arrow in Fig. 5). In contrast, the Bromo CO_2/S_t gas ratio is intermediate between the compositions of high-temperature gases from Merapi (4.3 to 6.3 at 850–900 °C; Allard, 1986; Allard et al., 1995, 2011) and Papandayan (2.9-3.0; Giggenbach et al., 2001), suggesting a magmatic (high-temperature) gas feeding source at Bromo. Thermodynamic computations based on the redox couples H_2/H_2O and H_2S/SO_2 (Fig. 3) also concur to suggest that Bromo gas emissions originate from a high-temperature (~700 °C), likely magmatic source with relatively oxidising redox conditions intermediate between the FeO–Fe_{2O3} and Nickel–Nickel Oxide buffers (NNO) (oxygen fugacities of 10^{-17}–10^{-18} bars). We caution that this inferred temperature of ~700 °C (Fig. 3) does likely under-estimate the real magmatic source temperature, since it probably only records the temperature of final gas equilibration in the so-called "effective source region" (von Glasow, 2010). This is the region at the magma–air interface where high-temperature volcanic volatiles mix and last equilibrate with air components. In-plume processing of reduced species (H_2 and H_2S) during later (lower temperature) atmospheric transport and dilution will likely be kinetically limited (Aiuppa et al., 2007; Martin et al., 2009), allowing quenched high-temperature H_2/H_2O vs. H_2S/SO_2 redox equilibria to remain preserved in otherwise cold volcanic plumes (Aiuppa et al., 2011).

The novel compositional data for Bromo, in tandem with previous results for Merapi and Papandayan, suggest that high-temperature gases from the Java arc segment converge to a relatively narrower range of CO_2/S_t ratios of ~3 to ~6 (see gray band area in Fig. 5). The average volcanic gas CO_2/S_t ratio of 4.3, calculated by Hilton et al. (2002) based on analysis of 42 gas samples from 10 Indonesian volcanic centres (Fig. 5), falls right in the middle of this compositional range. We note that our Java's CO_2/S_t ratio interval of 3–6 lies at the upper end of the range of arc volcanic gases (Fischer, 2008), and is well above the "mean arc" CO_2/S_t ratio (of ~2) recently proposed by Shinohara (2013) for persistently degassing open-vent volcanoes similar to Bromo. These results thus claim for an unusually C-rich signature of Java volcanic gases, relative to "mean arc" composition, possibly due to larger involvement of slab- or crustal-derived fluids (compared to other arc segments). We caution, however, that a larger gas dataset (than currently available) would be needed to more fully characterise variations in CO_2 origin and abundance (relative to sulphur) along the arc. For example, the high-temperature volcanic gases vented at Krakatau, right west of Java, are substantially more CO_2-poor (CO_2/S_t ratio of only ~0.4; Allard, 1986), implying that along-arc variations in gas chemistry can be important in Indonesia (as recently demonstrated in other, better studied arcs such as Central America; Aiuppa et al., 2014).

Our measured SO_2 flux of 164–168 t d^{-1} from Bromo is an order of magnitude higher than the low value (14 t d^{-1}) quoted by Andres and Kasgnoc (1998) and Shinohara (2013) (Fig. 6a). It is also much higher than the SO_2 output of 27.1 ± 9.5 t d^{-1} measured in June 2011 by Bani et al. (2013), using differential absorption spectroscopy (DOAS). Bani et al. (2013) outlined that their DOAS traverses did not cover the entire plume's cross-section and thus probably underestimated the actual SO_2 emission rate. Prior to our study and that of Bani et al. (2013), the SO_2 flux from Bromo had been measured in March 1995 (6, 22 and 22 t d^{-1}; GVP, 03/1995 – BGVN 20:03) and June 2004 (200 t d^{-1}; GVP, 05/2004 – BGVN 29:05). We note that the 2004 value is relatively close to our 2014 result. The overall range in these data suggests that Bromo's SO_2 source strength is not stable over time and that our September 2014 flux data does characterise a phase of increased degassing-seismic activity, such as previously mentioned. Clearly, better quantification of the time-averaged SO_2 emission rate from Bromo requires more frequent measurements in future. We argue, in particular, that the SO_2 fluxes may result particularly increased during the (relatively frequent) eruptive episodes of the volcano. For example, satellite-based UV observations (Carn et al., 2014 and 2015, pers. comm.) suggest a Bromo's time-averaged SO_2 flux of ~700 t d^{-1} for 2010–2014, a period encompassing the 2010–2012 eruptive episode (GVP; CVGHM Reports). Comparison between satellite- (OMI) and

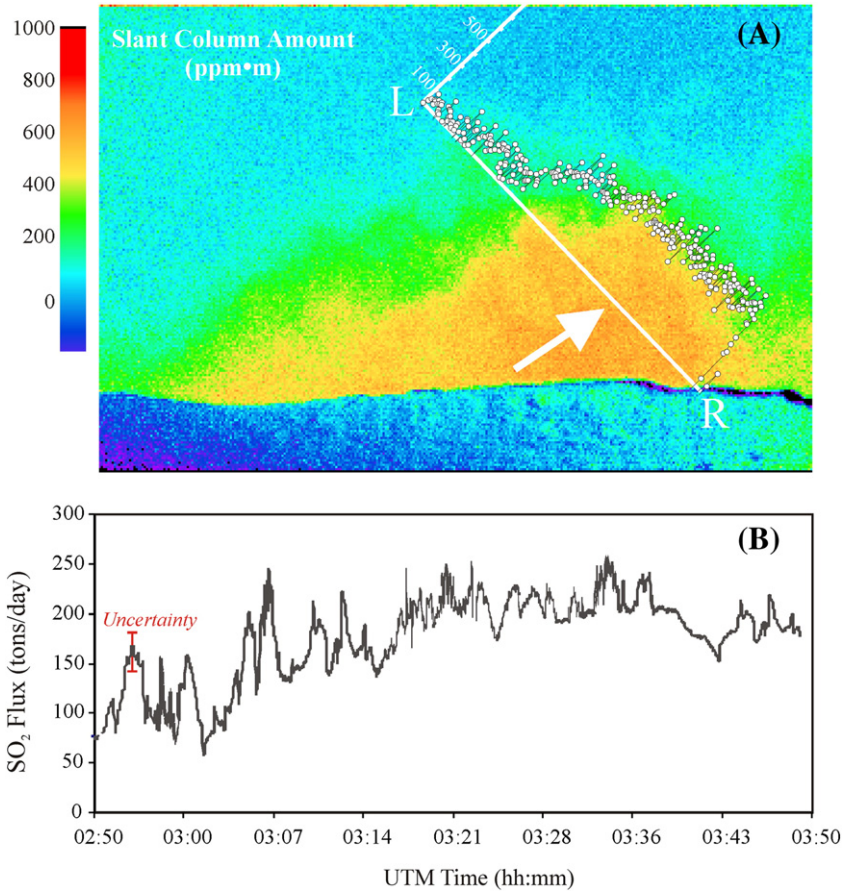

Fig. 4. (A) The Bromo plume seen is a UV camera image captured on September 20 at ~3.10 am local time. Pseudo-colours indicate SO_2 column amounts in the plume—in ppm m (see vertical colour bar for scale). A typical slant column amount cross section (from L to X in the image) is shown, from which integration the ICA (integrated column amount) was derived. The arrow stands for the plume transport direction. (B) A 1 h time-series of SO_2 flux emissions from Bromo (from 20 September, 2014). The red error bar demonstrates ±25% relative uncertainty on individual SO_2 flux data.

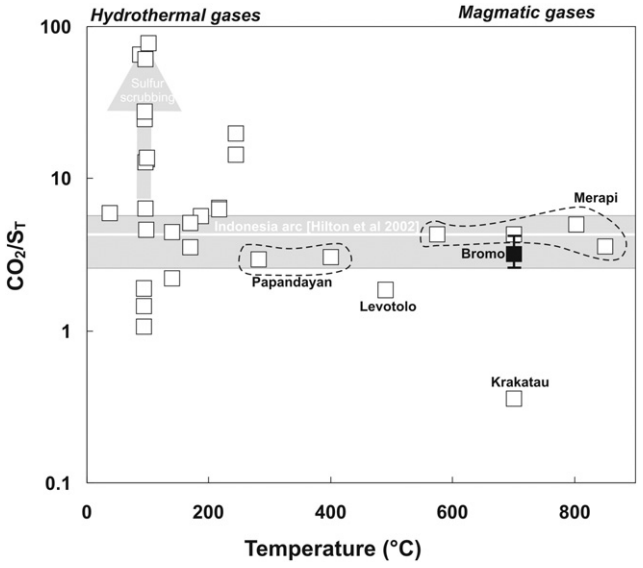

Fig. 5. Scatter plot of CO_2/S_t ratios in Indonesian volcanic gas emissions versus their discharge temperature. Low-temperature gases exhibit highly scattered CO_2/S_t ratios, as seen in other arc segments (e.g., Central America; Aiuppa et al., 2014), reflecting the role of gas-water rock reactions (gas scrubbing). High-temperature gases from the Java arc segment, including our novel Bromo data, converge to a narrower range of CO_2/S_t ratios (gray band area), that encompasses the Indonesian arc mean of Hilton et al (2002) (CO_2/S_t ratio of 4.3). Data source (except Bromo, this study): compilation of Indonesian gas sample of Pfeffer (2007).

ground-based (UV camera) surveys seems to suggest, therefore, that eruptive periods may release a factor ~3 more SO_2 than quiescent periods (our present study). We caution, however, that the higher emission rates from satellite observations may be biassed towards more explosive periods of activity from Bromo; with less intense (lower altitude) passive emissions, though dominant on the long-term, remaining undetected (or, at least, poorly detected) from space.

Our 2014 flux value ranks Bromo as a typical volcanic arc emitter, sitting in the central portion of the global volcanic SO_2 flux population (see Fig. 6a). In terms of SO_2 emission, Bromo is intermediate between the two largest Indonesian volcanoes yet measured, Merapi (time-average flux of 120 ± 30 t d^{-1} over three decades, range from 50 to >450 t/d; Allard, 1986; Allard et al., 1995, 2011; Surono et al., 2012) and Anak Krakatau (190 ± 65 t d^{-1}; Bani et al., 2015). Recently, Smekens et al. (2015) reported a first SO_2 flux measurement at Semeru volcano (Fig. 1d), just south of Bromo, with an estimated average daily emission of 22-71 t d^{-1}. They demonstrated that a substantial fraction (35–65%) of this SO_2 release occurs during short-lived periodic explosive events, while passive emissions in between the explosions contribute 9-50 t d^{-1}. Although quantitative comparison of these and our results is limited by observations having been made in different periods (May–June 2013 at Semeru and September 2014 at Bromo), it appears that Bromo's emissions may be 2–7 times higher than those of Semeru, suggesting that Bromo could make a significant (dominant?) contribution to the volcanic SO_2 emissions detected by satellites over the Tengger–Semeru massif (Carn et al., 2014).

The fluxes of other volatile species (H_2O, CO_2, H_2S and H_2) released by open-vent degassing at Bromo, quantified from our Multi-GAS data

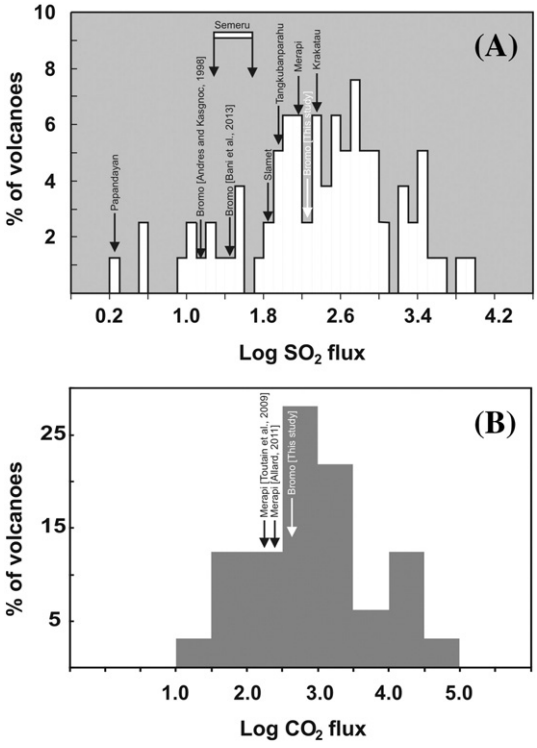

Fig. 6. (A) Frequency diagram of LogSO_2 emissions from persistent volcanic gas sources. The diagram plots the percentage (%) of persistently degassing volcanoes on earth falling within each LogSO_2 flux category, and was compiled from the global volcanic gas dataset of Shinohara (2013), except for Merapi (Allard et al., 2011), Semeru (Smekens et al.,2015), Anak Krakatau (Bani et al., 2015) and Bromo (Bani et al., 2013 and this study). The arrows indicate LogSO_2 flux values for individual Indonesian volcanoes; (B) Frequency diagram of LogCO_2 emissions from persistent volcanic sources. The diagram plots the percentage (%) of persistently degassing volcanoes on earth falling within each LogCO_2 flux category, and was drawn using the dataset of Aiuppa (2015) (an updated version of the global volcanic dataset compiled by Burton et al., 2013). The arrows demonstrate LogCO_2 flux values for individual Indonesian volcanoes.

(Table 1) and UV camera-based SO_2 flux values, are reported in Table 2. Gas fluxes are evaluated from the Multi-GAS and UV camera data sets simultaneously recorded during intervals A and C on September 20 and 21, respectively. We also report average flux values based on the mean gas composition (Table 1) and the mean SO_2 flux of 166 ± 38 t d^{-1}. The flux differences for the two days merely reflects the observed difference in gas composition and especially the higher water content of gases emitted on September 21 (Table 1). The H_2O flux from Bromo is estimated to range between 2630 ± 770 and 7380 ± 2540 t d^{-1}, with an average at 4700 ± 2300 t d^{-1}. Given the unclear, possibly meteoric H_2O-rich gas signature measured on September 21, we safely consider that the lower flux of ca. 2600 ± 800 t d^{-1} for September 20 better represents Bromo's magmatic emission. For comparison, the time-averaged H_2O emission from a typical arc volcano such as Stromboli, in Italy, has been evaluated at ~3550 t d^{-1} (Allard et al., 2008), while Mt. Etna emits ~3 times more H_2O on average (Aiuppa et al., 2008). Bromo's volcanic emission of CO_2 averages 460 ± 80 t d^{-1} (range: 390 ± 70 to 570 ± 200 t d^{-1}), which is in the intermediate range for the (few, to-date) measured volcanic CO_2 emitters (Burton et al., 2013; Aiuppa, 2015) (Fig. 6b). The only well documented Indonesian volcano to compare with is Merapi, where the plume CO_2 output averages 350 t d^{-1} (Allard et al., 1995; 2011), but where summit soil degassing of magma-derived CO_2 adds another ~230 t/d (Toutain et al., 2009). Finally, we show (Table 2) that Bromo also emits significant amounts of H_2S (25 ± 12 t d^{-1}) and H_2 (1.1 ± 0.8 t d^{-1}). The total flux of gas from Bromo in September 2014 thus averaged about 3300 t d^{-1} which, relying on future melt inclusion studies, could allow to assess the amount of involved magma.

6. Summary

We demonstrate that in late September 2014 Bromo volcano, in east Java, was daily emitting about 3300 tons of H_2O-rich volcanic gases through open-vent magma degassing. Bromo gas composition is dominated by water (H_2O/SO_2 ratio of 100 ± 50) and has a CO_2/S_t mean ratio (3.2) within the compositional range for high-temperature gas emissions from other Javanese volcanoes. Our measurements, which refer to a period of elevated quiescent (passive) degassing associated with increasing seismicity, constrain a SO_2 flux of 166 ± 38 t d^{-1}, in the upper range of the very few previous ground-based measurements. At the other extreme, using satellite-based UV imaging Carn et al. (2014 and 2015, pers. comm.) estimated a time-averaged SO_2 flux of ~700 t d^{-1} in 2010-2014, >3 times more than reported in our present study. We highlight that such a higher emission rate from satellite survey may however be biassed by being limited to the phases of eruptive activity and probably intense degassing that occurred at Bromo in 2010–2102. Otherwise, we show that Bromo ranks amongst the main volcanic sources of SO_2 and other gases in Indonesia, and may contribute a prevalent fraction of the space-detected SO_2 emissions from the Tengger-Semeru volcanic complex. We thus conclude that longer-term observations than reported here (2 days) would be required to better understand the long-term behaviour and volcano-related gas emissions of Bromo. The easy accessibility of the volcano's summit, combined with the persistent degassing activity, makes Bromo a particularly suitable site for setting up of a ground-based permanent gas monitoring system, eventually with an automated Multi-GAS. More generally, we highlight the need for new gas measurements on various volcanoes in Indonesia, in order to better include the contribution of this very active volcanic region into global volcanic gas budgets.

Acknowledgements

The research leading to these results has received funding from the European Research Council under the European Union's Seventh Framework Programme (FP7/2007/2013)/ERC grant agreement n 305377 (PI, Aiuppa).

References

Aiuppa, A., 2015. Volcanic gas monitoring. In: Schmidt, A., Fristad, K.E., Elkins-Tanton, L.T. (Eds.), Volcanism and Global Environmental Change. Cambridge University Press, pp. 81–96 http://dx.doi.org/10.1017/CBO9781107415683.009.

Aiuppa, A., Federico, C., Giudice, G., Gurrieri, S., 2005. Chemical mapping of a fumarolic field: La Fossa Crater, Vulcano Island (Aeolian Islands, Italy). Geophys. Res. Lett. 32 (13), L13309. http://dx.doi.org/10.1029/2005GL023207.

Aiuppa, A., et al., 2007. The tropospheric processing of acidic gases and hydrogen sulphide in volcanic gas plumes as inferred from field and model investigations. Atmos. Chem. Phys. 7, 1441–1450.

Aiuppa, A., Giudice, G., Gurrieri, S., Liuzzo, M., Burton, M., Caltabiano, T., et al., 2008. Total volatile flux from Mount Etna. Geophys. Res. Lett. 35 (L24302), L243–L252.

Aiuppa, A., Shinohara, H., Tamburello, G., Giudice, G., Liuzzo, M., Moretti, R., 2011. Hydrogen in the gas plume of an open-vent volcano, Mount Etna, Italy. J. Geophys. Res. B: Solid Earth 116 (10), B10204.

Aiuppa, A., Giudice, G., Liuzzo, M., Tamburello, G., Allard, P., Calabrese, S., Chaplygin, I., Mc Gonigle, A.J.S., Taran, Y., 2012. First volatile inventory for Gorely volcano, Kamchatka. Geophys. Res. Lett. 39, L06307. http://dx.doi.org/10.1029/2012GL051177.

Aiuppa, A., Tamburello, G., Di Napoli, R., Cardellini, C., Chiodini, G., Giudice, G., Grassa, F., Pedone, M., 2013. First observations of the fumarolic gas output from a restless caldera: Implications for the current period of unrest (2005–2013) at Campi Flegrei. Geochem. Geophys. Geosyst. 14, 4153–4169.

Aiuppa, A., Robidoux, P., Tamburello, G., Conde, V., Galle, B., Avard, G., Bagnato, E., De Moor, J.M., Martínez, M., Muñóz, A., 2014. Gas measurements from the Costa Rica–Nicaragua volcanic segment suggest possible along-arc variations in volcanic gas chemistry. Earth Planet. Sci. Lett. 407, 134–147.

Allard, P., 1986. Isotope geochemistry and origins of water, carbon and sulfur in volcanic gases: rift zones, continental margins and island arcs (State Thesis), Paris VII University (340 pp., (in French)).

Allard, P., Carbonnelle, J., Dajlevic, D., Métrich, N., Sabroux, J.-C., 1995. Volatile source and magma degassing budget of Merapi volcano: evidence from high-temperature gas emissions and crystal melt inclusions. Merapi Int. Decade Volcano Workshop. UNESCO/Volcanological Survey of Indonesia, Yogyakarta, pp. 16–17.

Allard, P., Aiuppa, A., Burto, N.M., Caltabiano, T., Federico, C., Salerno, G., La Spina, A., 2008. Crater Gas Emissions and the Magma Feeding System of Stromboli Volcano. In:

Calvari, S., Inguaggiato, S., Puglisi, G., Ripepe, M., Ros, M. (Eds.), Learning from Stromboli Volcano: An Integrated Study of the 2002–2003 Eruption. AGU Geophys. Monograph. Series 182, pp. 65–80. http://dx.doi.org/10.1029/GM182 (Washington D.C., Chap. 1.5).

Allard, P., Metrich, N., Sabroux, J.C., 2011. Volatile and magma supply to standard eruptive activity at Merapi volcano, Indonesia. Geophys. Res. Abstr. 13 (EGU2011-13522).

Andres, R.J., Kasgnoc, A.D., 1998. A time-averaged inventory of subaerial volcanic sulfur emissions. J. Geophys. Res. 103 (D19), 25,251–25,261.

Bani, P., Oppenheimer, C., Allard, P., Shinohara, H., Lardy, M., Garaebiti, E., 2012. First estimate of volcanic SO_2 budget for Vanuatu island arc. J. Volcanol. Geotherm. Res. 211–212, 36–46.

Bani, P., Surono, Hendrasto, M., Gunawan, H., Primulyana, S., 2013. Sulfur dioxide emissions from Papandayan and Bromo, two Indonesian volcanoes. Nat. Hazards Earth Syst. Sci. 13, 2399–2407.

Bani, P., Normier, A., Bacri, C., Gunawan, H., Hendrasto, M., Surono, Tsanev V., 2015. First evaluation of sulfur dioxide degassing from Anak Krakatau volcano, Indonesia. J. Volcanol. Geotherm. Res. 302, 237–241.

Burton, M.R., Sawyer, G.M., Granieri, D., 2013. Deep carbon emissions from volcanoes. Rev. Mineral. Geochem. 75 (1), 323–354.

Burton, M.R., Prata, F., Platt, U., 2015. Volcanological applications of SO_2 cameras. J. Volcanol. Geotherm. Res. 300, 2–6.

Carn, S.A., Pyle, D.M., 2001. Petrology and geochemistry of the Lamongan volcanic field, East Java, Indonesia: primitive Sunda arc magmas in an extensional tectonic setting? J. Petrol. 42, 1643–1683.

Carn, S.A., Flower, V.J.B., Telling, J.W., Yang, K., 2014. Satellite-Based Monitoring of Global Volcanic Degassing, Cities on Volcanoes 8, Yogyakarta, Indonesia, Sep 9–13.

Fischer, T.P., 2008. Fluxes of volatiles (H_2O, CO_2, N_2, Cl, F) from arc volcanoes. Geochem. J. 42, 21–38.

Giggenbach, W.F., et al., 2001. Evaluation of results from the fourth and fifth IAVCEI field workshops on volcanic gases, Vulcano island, Italy and Java, Indonesia. J. Volcanol. Geotherm. Res. 108 (1-4), 157–172.

Global Volcanism Program, 2012. Report on Tengger Caldera (Indonesia). In: Wunderman, R (Ed.), Bulletin of the Global Volcanism Network 37:10. Smithsonian Institution. http://dx.doi.org/10.5479/si.GVP.BGVN201210-263310.

Gottschämmer, E., 1999. Volcanic tremor associated with eruptive activity at Bromo Volcano. Ann. Geofis. 42, 465–481.

Gottschämmer, E., Surono, 2000. Locating tremor and shock sources recorded at Bromo Volcano. J. Volcanol. Geotherm. Res. 101, 199–209.

Hilton, D.R., Fischer, T.P., Marty, B., 2002. Noble gases and volatile recycling at subduction zones. Rev. Mineral. Geochem. 47.

Kantzas, E.P., McGonigle, A.J.S., Tamburello, G., Aiuppa, A., Bryant, R.G., 2010. Protocols for UV camera volcanic SO_2 measurements. J. Volcanol. Geotherm. Res. 194, 55–60. http://dx.doi.org/10.1016/j.jvolgeores.2010.05.003.

Kern, C., Kick, F., Lubcke, P., Vogel, L., Wohrbach, M., Platt, U., 2010. Theoretical description of functionality, applications and limitations of SO_2 cameras for the remote sensing of volcanic plumes. Atmos. Meas. Tech. 3, 733–749. http://dx.doi.org/10.5194/amt-3-733-2010.

Kern, C., Werner, C., Elias, T., Sutton, A.J., Lubcke, P., 2013. Applying UV cameras for SO_2 detection to distant or optically thick volcanic plumes. J. Volcanol. Geotherm. Res. 262, 80–89.

Martin, R.S., Roberts, T.J., Mather, T.A., Pyle, D.M., 2009. The implications of H_2S and H_2 stability in high-T mixtures of magmatic and atmospheric gases for the production of oxidized trace species (e.g., BrO and NOx). Chem. Geol. 263, 143–150.

McCormick, B.T., Edmonds, M., Mather, T.A., Carn, S.A., 2012. First synoptic analysis of volcanic degassing in Papua New Guinea. Geochem. Geophys. Geosyst. 13, Q03008. http://dx.doi.org/10.1029/2011GC003945.

McGonigle, A.J.S., Oppenheimer, C., Tsanev, V.I., Saunder, S., Mulina, K., Tohui, S., Bosco, J., Nahou, J., Kuduon, J., Taranu, F., 2004. Sulphur dioxide fluxes from Papua New Guinea's volcanoes. Geophys. Res. Lett. 31, L08606. http://dx.doi.org/10.1029/2004GL019568.

Mori, T., Burton, M., 2006. The SO_2 camera: a simple, fast and cheap method for ground-based imaging of SO_2 in volcanic plumes. Geophys. Res. Lett. 33, L24804. http://dx.doi.org/10.1029/2006GL027916.

Moussallam, Y., Oppenheimer, C., Aiuppa, A., Giudice, G., Moussallam, M., Kyle, P., 2012. Hydrogen emissions from Erebus volcano, Antarctica. Bull. Volcanol. 74 (9), 2109–2120. http://dx.doi.org/10.1007/s00445-012-0649-2.

Mulyadi, E., 1992. Le complexe de Bromo-Tengger Est Java, Indonesie Etude structurale et volcanologique (These) University Blaise Pascal, Clermont-Ferrand, France.

Nho, E.Y., Le Cloarec, M.-F., Ardouin, B., Tjetjep, W.S., 1996. Source strength assessment of volcanic trace elements emitted from the Indonesian arc. J. Volcanol. Geotherm. Res. 74, 121–129.

Oppenheimer, C., Fischer, T., Scaillet, B., 2014. Volcanic Degassing: Process and Impact in Treatise on Geochemistry. In: Holland, H.D., Turekian, K.K. (Eds.), Second edition Elsevier, Oxford, pp. 111–179 http://dx.doi.org/10.1016/B978-0-08-095975-7.00304-1.

Pfeffer, M.A., 2007. The Relative Influences of Volcanic and Anthropogenic Emissions on Air Pollution in Indonesia as Studied With a Regional Atmospheric Chemistry and Climate Model. Reports on Earth System Science. Max Planck Institute for Meteorology, Hamburg.

Shinohara, H., 2005. A new technique to estimate volcanic gas composition: plume measurements with a portable multi-sensor system. J. Volcanol. Geotherm. Res. 143, 319–333.

Shinohara, H., 2013. Volatile flux from subduction zone volcanoes: insights from a detailed evaluation of the fluxes from volcanoes in Japan. J. Volcanol. Geotherm. Res. 268, 46–63.

Simkin, T., Siebert, L., 1994. Volcanoes of the World. 2nd ed. Geoscience Press for the Smithsonian Institution, Tucson (Xi, 349 pp.).

Smekens, J.F., Clarke, A.B., Burton, M.R., Harijoko, A., Wibowo, H.E., 2015. SO_2 emissions at Semeru volcano, Indonesia: characterization and quantification of persistent and periodic explosive activity. J. Volcanol. Geotherm. Res. 300, 121–128.

Surono, et al., 2012. The 2010 explosive eruption of Java's Merapi volcano—a '100-year' event. J. Volcanol. Geotherm. Res. 241–242 (2012), 121–135. http://dx.doi.org/10.1016/j.jvolgeores.2012.06.018.

Symonds, R.B., Gerlach, T.M., Reed, M.H., 2001. Magmatic gas scrubbing: implications for volcano monitoring. J. Volcanol. Geotherm. Res. 108, 303–341.

Tamburello, G., 2015. Ratiocalc: software for processing data from multicomponent volcanic gas analyzers. Comput. Geosci. 82, 63–67.

Tamburello, G., Kantzas, E.P., McGonigle, A.J.S., Aiuppa, A., 2011. Vulcamera: a program for measuring volcanic SO2 using UV cameras. Ann. Geophys. 54 (2), 219–221. http://dx.doi.org/10.4401/ag-518.

Tamburello, G., Aiuppa, A., Kantzas, et al., 2012. Passive vs. active degassing modes at an open-vent volcano (Stromboli, Italy). Earth Planet. Sci. Lett. 359–360, 106–116.

Tamburello, G., Aiuppa, A., Mcgonigle, A.J.S., Allard, P., Cannata, A., Kantzas, E.P., 2013. Periodic volcanic degassing behavior: the Mount Etna example. Geophys. Res. Lett. 40, 4818–4822. http://dx.doi.org/10.1002/grl.50924.

Toutain, J.-P., Sortino, F., Baubron, J.-C., Richon, P., Surono, Sumarti, S., Nonell, A., 2009. Structure and CO_2 budget of Merapi volcano during inter-eruptive periods. Bull. Volcanol. 71 (7), 815–826. http://dx.doi.org/10.1007/s00445-009-0266-x.

van Gerven, M., Pichler, H., 1995. Some aspects of the volcanology and geochemistry of the Tengger Caldera, Java, Indonesia: eruption of a K-rich tholeiitic series. J. SE Asian Earth Sci. 11–2, 125–133.

von Glasow, R., 2010. Atmospheric chemistry in volcanic plumes. PNAS 107–15, 6594–6599 (www.pnas.org/cgi/doi/10.1073/pnas.0913164107).

Whitford, D.J., Nicholls, I.A., Taylor, S.R., 1979. Spatial variations in the geochemistry of quaternary lavas across the Sunda Arc in Java and Bali. Contrib. Mineral. Petrol. 70, 341–356.